Toward an Optimized Global-in-Time Schwarz Algorithm for Diffusion Equations with Discontinuous and Spatially Variable Coefficients, Part 1: The Constant Coefficients Case

Florian Lemarié, Laurent Debreu, Eric Blayo

TOWARD AN OPTIMIZED GLOBAL-IN-TIME SCHWARZ ALGORITHM FOR DIFFUSION EQUATIONS WITH DISCONTINUOUS AND SPATIALLY VARIABLE COEFFICIENTS

PART 1 : THE CONSTANT COEFFICIENTS CASE

FLORIAN LEMARIÉ*, LAURENT DEBREU†, AND ERIC BLAYO‡

Abstract. In this paper we present a global-in-time non-overlapping Schwarz method applied to the one dimensional unsteady diffusion equation. We address specifically the problem with discontinuous diffusion coefficients, our approach is therefore especially designed for subdomains with heterogeneous properties. We derive efficient interface conditions by solving analytically the minmax problem associated with the search for optimized conditions in a *Robin-Neumann* case and in a *two-sided Robin-Robin* case. The performance of the proposed schemes are illustrated by numerical experiments.

Key words. optimized Schwarz methods, waveform relaxation, alternating and parallel Schwarz methods

AMS subject classifications. 65M55, 65F10, 65N22, 35K15

1. Introduction. Numerous geophysical phenomena, with a strong societal impact, involve the coupled ocean-atmosphere system; e.g., for climate change, tropical cyclones, or sea-level rise predictions. To get a good depiction of the complex air-sea dynamics it is often necessary to couple atmospheric and oceanic computational simulation models. However, connecting the two model solutions at the air-sea interface is a difficult problem which is presently often addressed in a simplified way from a mathematical point of view. Indeed, with the *ad-hoc* coupling methods currently in use, the fluxes exchanged by the two models are generally not in exact balance [16]. This may be one factor explaining the strong sensitivity of coupled solutions to the initial conditions or parameter values generally observed [22]. This kind of coupling raises a number of challenges in terms of numerical simulation since we are considering two highly turbulent fluids with widely different scales in time and space. It is thus natural to use some specific numerical treatment to match the physics of the two fluids at their interface. It is known that, even if numerical models are much more complicated, a simple one-dimensional diffusion equation is relevant to locally represent the turbulent mixing in the boundary layers encompassing the air-sea interface. The corresponding diffusion coefficients are given by an *eddy-viscosity* closure predicting spatially variable diffusion coefficients [20]. To perform this coupling in a more consistent way than *ad-hoc* methods, we propose here to adapt a global-in-time domain decomposition based on an optimized Schwarz method. This type of method is thoroughly described in [9] and designed thanks to the pioneering work of [12, 13]. Schwarz-like domain decomposition methods provide flexible and efficient tools for coupling models with non-conforming time and space discretizations [3, 10]. Transmission conditions of Robin type have been proposed in [18] to circumvent the divergence of the classical Schwarz method in the case of non-overlapping subdomains. Then, thanks to the free parameters associated to the use of Robin conditions, an

*Corresponding author, Institute of Geophysics and Planetary Physics, University of California at Los Angeles, 405 Hilgard Avenue, Los Angeles, CA 90024-1567, United States (florian@atmos.ucla.edu, phone : +1-310-8255402, fax : +1-310-206-3051).

†INRIA Grenoble Rhône-Alpes, Montbonnot, 38334 Saint Ismier Cedex, France and Jean Kuntzmann Laboratory, BP 53, 38041 Grenoble Cedex 9, France (laurent.debreu@imag.fr, phone : +33 4 76 51 48 60, fax : +33 4 76 63 12 63).

‡University of Grenoble, Jean Kuntzmann Laboratory, BP 53, 38041 Grenoble Cedex 9, France (eric.blayo@imag.fr, phone : +33 4 76 63 59 63, fax : +33 4 76 63 12 63).

optimization of the convergence speed has been proposed in [12] and [14] : this is the basis of the so called *optimized Schwarz methods* (OSM). This kind of method, originally introduced for stationary problems, has been extended to unsteady cases by adapting the waveform relaxation algorithms to provide a *global-in-time Schwarz method* [13, 15] (sometimes referred to as *Schwarz waveform relaxation*). This notion of optimization of the convergence speed is critical in the context of ocean-atmosphere coupling as the numerical codes involved are very expensive from a computational point of view. In the present series of two papers we intend to derive interface conditions leading to an efficient Schwarz coupling algorithm between two unsteady diffusion equations defined on non-overlapping subdomains. The convergence properties of this kind of problem have already been extensively studied in the case of a constant diffusion coefficient having the same value in all subdomains [8]. There exists a few asymptotic results in the case of coefficients with different constant values in the different subdomains [10] (in the more general case of advection-diffusion-reaction equations). In the present papers, we extend these studies to the general case of diffusion coefficients which vary in each subdomain, and whose values are different on both sides of the interface. In this first part, we consider the case of diffusion coefficients that do not vary spatially in each medium. We study a zeroth-order *two-sided* optimized method by considering two different Robin conditions on both sides of the interface. In the second paper [17], the emphasis is on the impact of the spatial variability of the coefficients on the convergence speed.

This first paper is organized as follows. In section 2, we recall the basics of optimized Schwarz methods in the framework of time evolution problems. Sections 3 and 4 are dedicated to the study of a diffusion problem with discontinuous, but piecewise constant, coefficients. In section 3 we analytically determine the solution of an optimization problem to improve the convergence speed of a simplified algorithm with only one Robin condition combined with a Neumann condition. In section 4, we address the more general case of *two-sided* optimized Robin-Robin transmission conditions determined through a thorough study of the behaviour of the convergence factor. Finally in section 5 some numerical results are shown to prove the efficacy of the optimized algorithms derived in previous sections.

2. Model problem and Optimized Schwarz Methods. Our guiding example is the one dimensional diffusion equation of a scalar u

$$\mathcal{L}u = \partial_t u - \partial_x(D(x)\partial_x u) = f \qquad \text{in } \Omega \times [0,T], \tag{2.1}$$

where Ω is a bounded domain defined as $\Omega =]-L_1, L_2[$, $(L_1, L_2 \in \mathbb{R}^+)$, and $D(x) > 0, x \in \Omega$. In practical applications L_1 would denote the bottom of the ocean (of the order of 5 km in the open ocean) while L_2 is typically the top of the troposphere (of the order of 15 km). This problem is supplemented by an initial condition

$$u(x,0) = u_0(x) \qquad x \in \Omega,$$

and boundary conditions

$$\mathcal{B}_1 u(-L_1,t) = g_1 \qquad \mathcal{B}_2 u(L_2,t) = g_2 \qquad t \in [0,T],$$

where $\mathcal{B}_1$ and $\mathcal{B}_2$ are two partial differential operators. In the whole paper we assume that $u_0 \in H^1(\Omega)$, $f \in L^2(0,T;L^2(\Omega))$, and $D(x)$ bounded in L^∞-norm. Note that in actual applications such assumptions are generally fulfilled. Existence and uniqueness results for this problem can be proved following [10], and are not discussed here.

2.1. Formulation of global-in-time Schwarz method. In the present study, we consider a case where the diffusion coefficient $D(x)$ has one discontinuity in Ω. This discontinuity is representative of the transition between two media with heterogeneous physical properties. In this case we can define two subdomains, each subdomain having its own diffusion

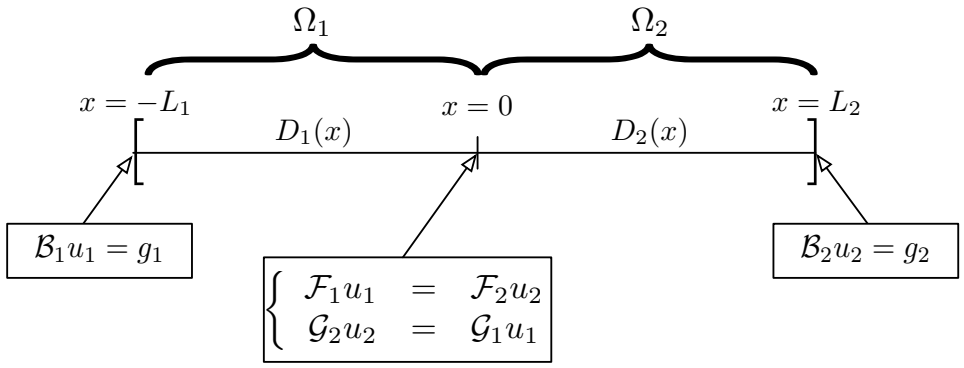

FIG. 2.1. *Decomposition of the spatial domain Ω into two non-overlapping subdomains.*

profile $D_j(x)$, $(j = 1, 2)$. This amounts to split Ω into two non-overlapping domains Ω_1 and Ω_2 (Fig. 2.1). Those subdomains communicate through their common interface $\Gamma = \{x = 0\}$ (note that there can be various reasons for such a splitting: different physics, parallelization and/or different numerical treatment requirements). We propose to use a non-overlapping global-in-time Schwarz algorithm to solve the corresponding coupling problem. This method consists in solving iteratively subproblems in $\Omega_1 \times [0, T]$ and $\Omega_2 \times [0, T]$ using as an interface condition at $x = 0$ the values computed at the previous iteration in the other subdomain. The operator $\mathcal{L}$ introduced in (2.1) is split into two operators $\mathcal{L}_j = \partial_t - \partial_x(D_j(x)\partial_x)$ restricted to Ω_j $(j = 1, 2)$. Introducing the operators $\mathcal{F}_1$, $\mathcal{F}_2$, $\mathcal{G}_1$ and $\mathcal{G}_2$ to define the interface conditions, the algorithm reads

(2.2)

$$\begin{cases} \mathcal{L}_1 u_1^k = f & \text{in } \Omega_1 \times [0,T] \\ u_1^k(x,0) = u_o(x) & x \in \Omega_1 \\ \mathcal{B}_1 u_1^k(-L_1,t) = g_1 & t \in [0,T] \\ \mathcal{F}_1 u_1^k(0,t) = \mathcal{F}_2 u_2^{k-1}(0,t) & \text{in } \Gamma \times [0,T] \end{cases} \quad \begin{cases} \mathcal{L}_2 u_2^k = f & \text{in } \Omega_2 \times [0,T] \\ u_2^k(x,0) = u_o(x) & x \in \Omega_2 \\ \mathcal{B}_2 u_2^k(L_2,t) = g_2 & t \in [0,T] \\ \mathcal{G}_2 u_2^k(0,t) = \mathcal{G}_1 u_1^k(0,t) & \text{in } \Gamma \times [0,T] \end{cases}$$

where $k = 1, 2, ...$ is the iteration number and where the initial guess $u_2^0(0, t)$ is given. Algorithm (2.2) corresponds to the so-called "multiplicative" form of the Schwarz method. If we replace the interface condition $\mathcal{G}_2 u_2^k = \mathcal{G}_1 u_1^k$ on Ω_2 by $\mathcal{G}_2 u_2^k = \mathcal{G}_1 u_1^{k-1}$ we obtain the "parallel" version of the algorithm. The multiplicative form converges more rapidly than the parallel one but prevents from solving subproblems in parallel (this problem can however be circumvented when we consider more than two subdomains). Interested readers may refer to [7] for further details regarding the different variants of the Schwarz method. Although the present study uses the multiplicative form of the algorithm, the theoretical results regarding the determination of optimized transmission conditions are also valid for the parallel form. Note that the usual algorithmic approach used by ocean-atmosphere climate models, as described in [4], generally corresponds to one (and only one) iteration of algorithm (2.2) (with $\mathcal{F}_j = \mathcal{G}_j = D_j(0)\partial_x,\ j = 1, 2$).

The primary role of operators $\mathcal{F}_j$ and $\mathcal{G}_j$ $(j = 1, 2)$ in (2.2) is to ensure a given consistency of the solution on the interface Γ. In our context we require the equality of the subproblems solutions and of their fluxes. The most natural choice to obtain such a connection consists in

choosing

$$\mathcal{F}_1 = D_1(0)\frac{\partial}{\partial x} \qquad \mathcal{F}_2 = D_2(0)\frac{\partial}{\partial x} \qquad \mathcal{G}_1 = \mathcal{G}_2 = Id.$$

However, as proposed in [18], the same consistency can be obtained using mixed boundary conditions of Robin type, leading to

$$\mathcal{F}_j = D_j(0)\frac{\partial}{\partial x} + \Lambda_1 \qquad \mathcal{G}_j = D_j(0)\frac{\partial}{\partial x} + \Lambda_2 \qquad (j = 1, 2). \tag{2.3}$$

This type of condition has the advantage to add operators Λ_1 and Λ_2 in the coupled problem. Those operators, if correctly chosen, can greatly improve the convergence speed of the corresponding algorithm [12]. Note that the Λ_j must also be carefully chosen to ensure the well-posedness of the problem. In this paper we focus on Robin-type transmission conditions since *Dirichlet-Neumann*-type algorithms converge generally quite slowly, except for large discontinuities between the coefficients D_2 and D_1 (it can easily be shown that the convergence rate is given by the square root of the ratio between D_1 and D_2).

At this point, we have formulated the coupling problem we want to address. The convergence properties of this kind of problem have been extensively studied in the case of constant and continuous diffusion coefficients [8]. There also exists a few results in the case of constant and discontinuous coefficients [10] in the more general case of an advection-diffusion-reaction problem. This latter study provides results for specific asymptotic cases that are discussed later in section 4.4. In this paper, we propose to investigate the problem with diffusion coefficients constant in each subdomain and discontinuous at the interface; i.e., $D_j(x) = D_j$, with $D_j > 0$ and $D_1 \neq D_2$. We prove the convergence of algorithm (2.2) and we determine optimal choices for the Λ_j operators, under some constraints on the parameters of the problem.

2.2. Convergence of the algorithm. A classical approach to demonstrate the convergence of algorithm (2.2) consists in introducing the error e_j^k between the exact solution $u^\star$ and the iterates u_j^k, $j = 1, 2$. By linearity, those errors satisfy homogeneous diffusion equations with homogeneous initial conditions. We denote the Fourier transform in time by $\widehat{g} = \mathcal{F}(g)$ for any $g \in L^2(\mathbb{R})$. Assuming that $T \to \infty$ and that all the functions are equal to zero for negative times, it can easily be shown that the errors $\widehat{e}_j^k$ in Fourier space satisfy a second-order ordinary differential equation in x

$$i\omega\widehat{e}_j^k - D_j\frac{\partial^2\widehat{e}_j^k}{\partial x^2} = 0 \qquad \text{for } x \in \Omega_j, \omega \in \mathbb{R}^*$$

with characteristic roots $\sigma_j^\pm = \pm\sqrt{\dfrac{|\omega|}{2D_j}}\left(1 + \dfrac{|\omega|}{\omega}i\right)$. Note that the particular case $\omega = 0$ would correspond to the existence of a stationary part in the error. However, since the error is initially zero, such a stationary part is also necessary zero. To study the convergence of algorithm (2.2), the domain Ω is usually supposed unbounded ($L_1, L_2 \to \infty$), thus leading to

$$\begin{cases} \widehat{e}_1^k(x,\omega) &= \alpha^k(\omega)e^{\sigma_1^+ x} & \text{for } x < 0, \omega \in \mathbb{R}^* \\ \widehat{e}_2^k(x,\omega) &= \beta^k(\omega)e^{\sigma_2^- x} & \text{for } x > 0, \omega \in \mathbb{R}^* \end{cases} \tag{2.4}$$

The validity of this assumption is discussed in [16]. The functions $\alpha(\omega)$ and $\beta(\omega)$ are determined using the Robin interface conditions at $x = 0$

$$\left\{ \begin{array}{rcl} (\ D_1\sigma_1^+ + \lambda_1)\alpha^k(\omega) & = & (\ D_2\sigma_2^- + \lambda_1)\beta^{k-1}(\omega) \\ (-D_2\sigma_2^- + \lambda_2)\beta^k(\omega) & = & (-D_1\sigma_1^+ + \lambda_2)\alpha^k(\omega) \end{array} \right. \tag{2.5}$$

where λ_j is defined as the *symbol* of operator Λ_j ($j = 1, 2$). A convergence factor ρ of the Schwarz algorithm (2.2) can be defined as

$$\rho(\omega) = \left| \frac{\widehat{e}_1^k(0,\omega)}{\widehat{e}_1^{k-1}(0,\omega)} \right| = \left| \frac{\widehat{e}_2^k(0,\omega)}{\widehat{e}_2^{k-1}(0,\omega)} \right|$$

Given (2.4), this amounts to $\rho(\omega) = \left|\alpha^k/\alpha^{k-1}\right| = \left|\beta^k/\beta^{k-1}\right|$. Using (2.5) we obtain

$$\rho(\omega) = \left| \frac{(\lambda_1(\omega) + D_2\sigma_2^-)}{(\lambda_1(\omega) + D_1\sigma_1^+)} \frac{(\lambda_2(\omega) - D_1\sigma_1^+)}{(\lambda_2(\omega) - D_2\sigma_2^-)} \right| \tag{2.6}$$

A more general derivation of the convergence factor for the case of an advection-diffusion-reaction problem with discontinuous coefficients can be found in [10]. At this point, we are not able to conclude on the convergence (or the divergence) of the corresponding algorithm because the operators Λ_j have not been explicitly determined. This is often a difficult task to choose them in an appropriate way. The main difficulty comes from the fact that the convergence factor is formulated in the Fourier space, meaning that we can only act on symbols λ_j and not directly on pseudo-differential operators Λ_j in physical space.

2.3. Optimized Schwarz Method. It is possible to find values λ_1 and λ_2 canceling the convergence factor (2.6) and therefore ensuring a convergence in exactly two iterations. Their expressions are

$$\lambda_1^{\text{opt}} = -D_2\sigma_2^- = \sqrt{\frac{|\omega|D_2}{2}}(1 + \frac{|\omega|}{\omega}i) \qquad \lambda_2^{\text{opt}} = D_1\sigma_1^+ = \sqrt{\frac{|\omega|D_1}{2}}(1 + \frac{|\omega|}{\omega}i) \tag{2.7}$$

These symbols correspond to so-called *absorbing conditions*. Unfortunately, since these optimal symbols are not polynomials in $i\omega$, the absorbing conditions are non-local in time in the physical space. The problem is thus to find local operators providing a good approximation of non-local ones. The aim is to find a polynomial form in $i\omega$ to approximate λ_j^{opt}. There are mainly two approaches for such an approximation [12]. The first one consists in a low frequency approximation, namely a Taylor expansion for a small ω. We decided not to adopt this approach because we want to be able to consider a wide range of frequencies. The second, and more sophisticated, approach is to solve a minimax problem to determine local operators that optimize the convergence speed over the full range of admissible frequencies $[\omega_{\min}, \omega_{\max}]$. For a zeroth-order approximation we look for values $\lambda_j^0 \in I\!R$ such that $\lambda_j^0 \approx \lambda_j^{\text{opt}}$. The λ_j^0 terms can be defined as the solution of the optimization problem

$$\min_{\lambda_1^0, \lambda_2^0 \in \mathbb{R}} \left(\max_{\omega \in [\omega_{\min}, \omega_{\max}]} \rho(\lambda_1^0, \lambda_2^0, \omega) \right) \tag{2.8}$$

Since we work on a discrete problem the frequencies allowed by our temporal grid range from $\omega_{\min} = \dfrac{\pi}{T}$ to $\omega_{\max} = \dfrac{\pi}{\Delta t}$, where Δt is the time step of the temporal discretization. The analytical resolution of problem (2.8) is not an easy task: the minimization of a maximum is known to be one of the most difficult problem in optimization theory [5]. Moreover, we

work on an optimization for two parameters λ_1^0 and λ_2^0 which substantially strengthens the difficulty. Some analytical results exist in the case of *two-sided* optimization for the 2D stationary diffusion equation [6, 19], and for the 2D Helmholtz equation [11]. In [10], for an advection-diffusion-reaction problem, the asymptotic solution of (2.8) for $\Delta t \to 0, \omega_{\min} = 0$, and a positive advection is found in two particular cases: first $\lambda_1^0 = \lambda_2^0$ (*one-sided*), and second $\lambda_1^0 \neq \lambda_2^0$ (*two-sided*) but $D_1 = D_2$. In this paper, we intend to study the complete minmax problem (2.8) in the general case $\lambda_1^0 \neq \lambda_2^0$ and $D_1 \neq D_2$. Solving numerically the minimax problem (2.8) is quite expensive from a computational point of view. Moreover this optimization must be performed for any change in the values of D_1 and D_2. That is why we intend to find an analytical solution in the case of a zeroth-order approximation of the absorbing conditions. This is done with two different sets of interface conditions, first in the *Neumann-Robin* case, and then in the *Robin-Robin* case.

The algorithm (2.2) with two-sided Robin conditions is well-posed for any choice of λ_1^0 and λ_2^0 such that $\lambda_1^0 + \lambda_2^0 > 0$. This result can be shown following the methodology based on a priori energy estimate, as described in [1] and [8].

3. Optimized Schwarz method with *Neumann-Robin* interface conditions. In this section, we assume that the solution in Ω_2 is subject to a Neumann boundary condition. The convergence speed of the Neumann-Robin algorithm is expected to be slower than the one obtained with a Robin-Robin algorithm. However this easier case is treated explicitly because it introduces several methodological aspects useful for the determination of the general Robin-Robin optimized interface conditions. Imposing a Neumann boundary condition to the solution u_2 on Γ corresponds to having $\Lambda_2 = 0$ in (2.3). The convergence factor ρ_{NR} (NR stands for "Neumann-Robin"), obtained from (2.6), reduces to

$$\rho_{\text{NR}} = \left| \frac{D_1\sigma_1^+}{D_2\sigma_2^-} \frac{(D_2\sigma_2^- + \lambda_1)}{(D_1\sigma_1^+ + \lambda_1)} \right| \tag{3.1}$$

THEOREM 3.1 (Optimized Robin parameter). *The analytical solution $\lambda_1^{0,\star}$ of the minimax problem*

$$\min_{\lambda_1^0 \in \mathbb{R}} \left(\max_{\omega \in [\omega_{\min}, \omega_{\max}]} \rho_{\text{NR}}(\lambda_1^0, D_1, D_2, \omega) \right)$$

is given by

$$\begin{aligned} \lambda_1^{0,\star} &= \frac{1}{2\sqrt{2}} \left\{ \left(\sqrt{D_2} - \sqrt{D_1} \right) \left(\sqrt{\omega_{\min}} + \sqrt{\omega_{\max}} \right) \right. \\ &+ \left. \sqrt{\left(\sqrt{D_2} - \sqrt{D_1} \right)^2 \left(\sqrt{\omega_{\min}} + \sqrt{\omega_{\max}} \right)^2 + 8\sqrt{D_1 D_2}\sqrt{\omega_{\min}\omega_{\max}}} \right\} \end{aligned}$$

Proof. : Introducing $\zeta = \sqrt{|\omega| D_1}$, $\gamma = \sqrt{D_2/D_1}$, $\lambda_1^0 = \left(\sqrt{\zeta_{\min}\zeta_{\max}/2} \right) p \quad (p \in \mathbb{R})$, and making explicit σ_1^+ and σ_2^- in (3.1), we obtain

$$\rho_{\text{NR}}(p, \boldsymbol{\zeta}) = \frac{1}{\gamma} \sqrt{\frac{(p - \gamma\boldsymbol{\zeta})^2 + \gamma^2\boldsymbol{\zeta}^2}{(p + \boldsymbol{\zeta})^2 + \boldsymbol{\zeta}^2}},$$

with $\boldsymbol{\zeta} = \zeta / \sqrt{\zeta_{\max}\zeta_{\min}}$. Moreover, to ensure the well-posedness of the algorithm we consider $\lambda_1^0 > 0$ (i.e.; $p > 0$). Defining an additional parameter $\mu = \sqrt{\zeta_{\max}/\zeta_{\min}}$, we thus get

that ζ varies between $\zeta_{\min} = \mu^{-1}$ and $\zeta_{\max} = \mu$. The aim is to optimize the convergence speed by finding $p^\star$, the solution of the minimax problem

$$\min_{p>0} \left(\max_{\zeta \in [\mu^{-1}, \mu]} \rho_{\text{NR}}(p, \zeta) \right).$$

We first study the behaviour of the derivative of ρ_{NR} with respect to ζ and p (with $\zeta \geq 0$ and $p \geq 0$). For the sake of simplicity we introduce the variable q defined by $q = p/\left(\gamma - 1 + \sqrt{1+\gamma^2}\right)$.

Restriction of the parameters range. We can easily show that

$$\text{Sign}\left(\frac{\partial \rho_{\text{NR}}}{\partial p}\right) = \text{Sign}\left(q - \zeta\right). \tag{3.2}$$

Looking at the sign of the derivative of ρ_{NR} with respect to p, we see that, for all values of ζ, ρ_{NR} is a decreasing function of p for $q < \zeta_{\min} = \mu^{-1}$, proving that $q^\star \geq \zeta_{\min}$. A similar argument shows that $q^\star \leq \zeta_{\max}$. This proves that the optimized parameter $q^\star$ satisfies

$$1/\mu \leq q^\star \leq \mu$$

Along with (3.2), this shows that the convergence factor has to be an increasing function of p at $\zeta = 1/\mu$ and a decreasing function of p at $\zeta = \mu$.

Equioscillation property. The sign of the derivative of ρ_{NR} with respect to ζ is given by

$$\text{Sign}\left(\frac{\partial \rho_{\text{NR}}}{\partial \zeta}\right) = \text{Sign}\left(\zeta - q\right).$$

This relation implies that ρ_{NR} has a local minima between $1/\mu$ and μ. The maximum value of the convergence factor is thus attained either at $\zeta = 1/\mu$ or at $\zeta = \mu$ (or both). If we assume $\rho_{\text{NR}}(p, 1/\mu) < \rho_{\text{NR}}(p, \mu)$ it is always possible to decrease the maximum value of $\rho_{\text{NR}}(p, \zeta)$ by increasing the value of p so that we must have $\rho_{\text{NR}}(p, 1/\mu) \geq \rho_{\text{NR}}(p, \mu)$. A similar argument shows that $\rho_{\text{NR}}(p, \mu) \geq \rho_{\text{NR}}(p, 1/\mu)$. The optimal parameter must thus satisfy the equioscillation property $\rho_{\text{NR}}(p^\star, 1/\mu) = \rho_{\text{NR}}(p^\star, \mu)$. After simple algebra, we find that $p^\star$ is solution of

$$(\gamma - 1)\left(\mu + 1/\mu\right) + \frac{2\gamma}{p^\star} - p^\star = 0.$$

If we introduce $v^\star = (1-\gamma)\left(\mu + 1/\mu\right)$, the unique positive solution of the equation $v^\star = \dfrac{2\gamma}{p^\star} - p^\star$ is given by $p^\star = \dfrac{1}{2}\left(-v^\star + \sqrt{8\gamma + (v^\star)^2}\right)$. After substitution of γ and μ, and multiplication of $p^\star$ by $\sqrt{\zeta_{\min}\zeta_{\max}/2}$ we retrieve the expected result for $\lambda_1^{0,\star}$. □

We find that the optimized convergence factor satisfies an equioscillation property. This concept of equioscillation property comes from the Chebyshev's alternant theorem (or equioscillation theorem). The similarities between the Chebyshev's theorem and Optimized Schwarz Method are clearly exposed in [2] and [6]. Two typical optimized convergence factors $\rho_{\text{NR}}^\star = \rho_{\text{NR}}(\lambda_1^{0,\star})$ are shown in Fig. 3.1 (left panel) for $\mu = 2$ and $\mu = 6$, with γ = 5. Note that the performance of the optimized algorithm is only function of the ratio γ between D_1 and D_2 and not of the actual values of those parameters. The same remark applies to the temporal frequencies $\omega_{\min}$ and $\omega_{\max}$; $\rho_{\text{NR}}^\star$ is only function of their ratio μ. It is also instructive to look at three particular cases: $\gamma \to 0^+$, $\gamma = 1$ and $\gamma \to \infty$.

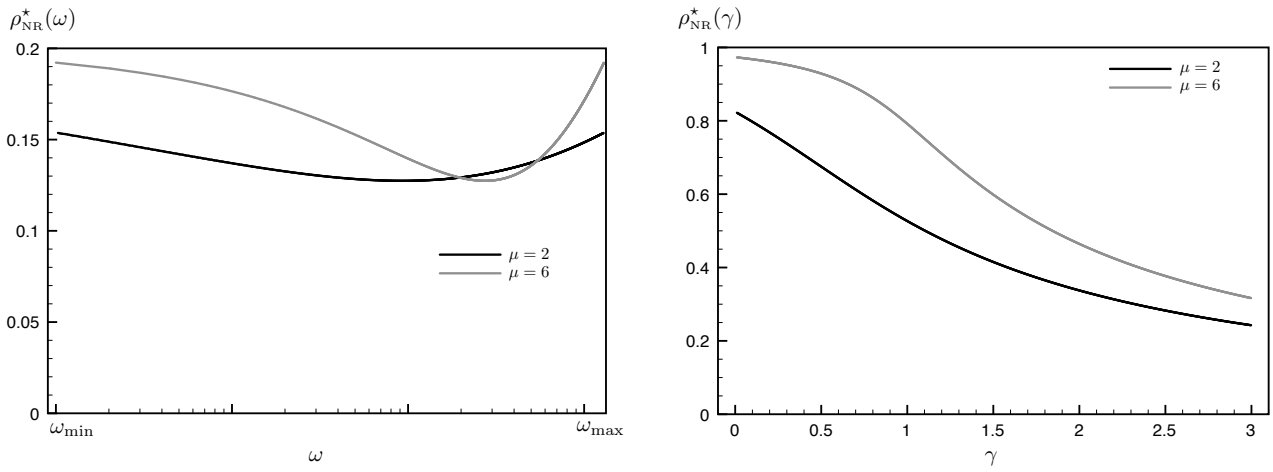

FIG. 3.1. *Behaviour of $\rho_{NR}(\lambda_1^{0,\star})$ with respect to ω, for $\gamma = 5$, $\mu = 2$ and $\mu = 6$ (left). Optimized convergence factor as a function of γ for $\mu = 2$ and $\mu = 6$ (right).*

- $\gamma \to 0^+$ $(D_1 \gg D_2)$

$$\lim_{\gamma\to 0^+} \rho^\star_{\mathrm{NR}} = \sqrt{1 - 2\left(\frac{\mu}{1+\mu^2}\right)^2}, \qquad \lim_{\gamma\to 0^+} \lambda_1^{0,\star} = 0, \qquad \text{with } \mu = \left(\frac{\omega_{\max}}{\omega_{\min}}\right)^{1/4}$$

The minimum value of the convergence factor is attained at $\mu = 1$ and is equal to $\sqrt{2}/2$. When μ is increased, the convergence is very slow. Indeed, we tend towards a Neumann-Neumann algorithm in this case.

- $\gamma = 1$ $(D_1 = D_2 = D)$

$$\rho^\star_{\mathrm{NR}} = \sqrt{1 - \frac{2\sqrt{2}\mu}{1+\mu(\mu+\sqrt{2})}}, \qquad \lambda_1^{0,\star} = \sqrt{D}\left(\omega_{\max}\omega_{\min}\right)^{1/4}$$

$\rho^\star_{\mathrm{NR}}$ approaches 1 when μ is increased. One can also remark that the optimal parameter $\lambda_1^{0,\star}$ is strictly the same than the one found in [8] in the Robin-Robin one-sided case.

- $\gamma \to +\infty$ $(D_1 \ll D_2)$

$$\lim_{\gamma\to+\infty} \rho^\star_{\mathrm{NR}} = 0, \qquad \lim_{\gamma\to+\infty} \lambda_1^{0,\star} = +\infty$$

When γ tends to $+\infty$, the convergence is very fast (the convergence factor approaches 0) and the optimal boundary condition tends towards a Neumann-Dirichlet operator.

Those results are illustrated by Fig. 3.1 (right panel). The efficiency of the Neumann-Robin algorithm is greatly improved when γ becomes large and μ becomes small. We continue this section by studying the asymptotic convergence rate for the discretized algorithm when the time step Δt goes to 0.

THEOREM 3.2 (Asymptotic performance). *For $D_2 > D_1$ (i.e., $\gamma > 1$), $\omega_{\max} = \dfrac{\pi}{\Delta t}$ and Δt goes to zero, the optimal Robin parameter given by Theorem 3.1 is*

$$\lambda_1^{0,\star} \approx \sqrt{2D_1}\left(\frac{\gamma-1}{2}\sqrt{\pi}\Delta t^{-1/2} + \frac{\gamma^2+1}{2(\gamma-1)}\sqrt{\omega_{\min}}\right)$$

and the asymptotic convergence of the optimized Neumann-Robin algorithm is

$$\max_{\omega_{\min}\leq\omega\leq\frac{\pi}{\Delta t}} \rho_{NR}(\lambda_1^{0,\star},\omega) = \frac{1}{\gamma}\left(1 - \frac{(\gamma+1)}{(\gamma-1)}\sqrt{\frac{\omega_{\min}}{\pi}}\Delta t^{1/2}\right) + O(\Delta t)$$

We conclude that zeroth-order optimized Neumann-Robin boundary conditions are efficient when the Robin condition is imposed at the boundary of the domain with the smaller diffusion coefficient (Ω_1 here). In this case, the asymptotic convergence factor $\rho_{\text{NR}}^\star$ is of the form $\sqrt{D_1/D_2}\left(1 - O(\Delta t^{1/2})\right)$ for small Δt. In the next section, we study the zeroth-order two-sided Robin-Robin boundary conditions.

4. OSM for a diffusion problem with discontinuous (but constant) coefficients: two-sided Robin transmission conditions. In this section we optimize the conditions on both sides of the interface to get a faster convergence speed whatever the value of the discontinuity γ in the coefficient values at the interface. By keeping the notations ζ, $\boldsymbol{\zeta}$, μ and γ defined in the previous section and by approximating λ_1^{opt} and λ_2^{opt} respectively by $\lambda_1^0 = \sqrt{\dfrac{\zeta_{\min}\zeta_{\max}}{2}}\, p_2$ and $\lambda_2^0 = \sqrt{\dfrac{\zeta_{\min}\zeta_{\max}}{2}}\, p_1$ the convergence factor ρ_{RR} reads

$$\rho_{\text{RR}}(p_1,p_2,\boldsymbol{\zeta}) = \sqrt{\frac{\left((p_1-\boldsymbol{\zeta})^2+\boldsymbol{\zeta}^2\right)\left((p_2-\gamma\boldsymbol{\zeta})^2+\gamma^2\boldsymbol{\zeta}^2\right)}{\left((p_1+\gamma\boldsymbol{\zeta})^2+\gamma^2\boldsymbol{\zeta}^2\right)\left((p_2+\boldsymbol{\zeta})^2+\boldsymbol{\zeta}^2\right)}}$$

We can easily demonstrate that, for nonnegative fixed values of $\boldsymbol{\zeta}$ and γ and for $p_1, p_2 > 0$ we have $\rho_{\text{RR}}(p_1,p_2,\boldsymbol{\zeta}) < \rho_{\text{RR}}(-p_1,-p_2,\boldsymbol{\zeta})$, as well as $\rho_{\text{RR}}(p_1,p_2,\boldsymbol{\zeta}) < \rho_{\text{RR}}(p_1,-p_2,\boldsymbol{\zeta})$, and $\rho_{\text{RR}}(p_1,p_2,\boldsymbol{\zeta}) < \rho_{\text{RR}}(-p_1,p_2,\boldsymbol{\zeta})$. Those three inequalities show that we can restrict our study to strictly positive values of p_1 and p_2 (note that $p_1 = 0$ or $p_2 = 0$ corresponds to the *Neumann-Robin* case. The restriction of the parameter range to strictly positive values ensures that $\lambda_1^0 + \lambda_2^0 > 0$, and thus that the corresponding porblem is well-posed. In the following, we assume that $\gamma \geq 1$. The Robin-Robin problem being now symmetric, optimal parameters p_1 and p_2 for the case $\gamma \leq 1$ can be obtained by switching optimal values for the case $\gamma \geq 1$. As done previously we choose the p_1 and p_2 values by solving the optimisation problem

$$\min_{p_1,p_2>0}\left(\max_{\boldsymbol{\zeta}\in[\mu^{-1},\mu]} \rho_{\text{RR}}(p_1,p_2,\boldsymbol{\zeta})\right) \tag{4.1}$$

4.1. Behaviour of the convergence factor with respect to the Robin parameters. First, we study the behaviour of ρ_{RR} with respect to the parameters p_1 and p_2. We introduce two new parameters q_1 and q_2 defined by

$$q_1 = \frac{p_1}{1-\gamma+\sqrt{1+\gamma^2}} \qquad q_2 = \frac{p_2}{\gamma-1+\sqrt{1+\gamma^2}}$$

We can demonstrate that for $\gamma \geq 1$ and $q_1 \leq q_2$, we have $\rho_{\text{RR}}(p_1,p_2,\boldsymbol{\zeta}) \leq \rho_{\text{RR}}(p_2,p_1,\boldsymbol{\zeta})$. This proves that the optimal parameters satisfy $q_1^\star \leq q_2^\star$. This implies that in turn $p_1 \leq p_2$ and that $p_1 < p_2$ if $\gamma > 1$. This immediately proves that *one-sided* ($p_1 = p_2$) Robin-Robin boundary conditions are not optimal as soon as $\gamma > 1$.

Restriction of the parameters range. Noting that $\text{Sign}\left(\frac{\partial \rho_{\text{RR}}}{\partial p_1}\right) = \text{Sign}(q_1 - \boldsymbol{\zeta})$ and $\text{Sign}\left(\frac{\partial \rho_{\text{RR}}}{\partial p_2}\right) = \text{Sign}(q_2 - \boldsymbol{\zeta})$ implies

$$\begin{array}{ll} \frac{\partial \rho_{\text{RR}}}{\partial p_1} > 0 \text{ when } \boldsymbol{\zeta} < q_1 & \frac{\partial \rho_{\text{RR}}}{\partial p_1} < 0 \text{ when } \boldsymbol{\zeta} > q_1 \\ \frac{\partial \rho_{\text{RR}}}{\partial p_2} > 0 \text{ when } \boldsymbol{\zeta} < q_2 & \frac{\partial \rho_{\text{RR}}}{\partial p_2} < 0 \text{ when } \boldsymbol{\zeta} > q_2 \end{array} \tag{4.2}$$

Looking at the sign of the derivatives of ρ_{RR} with respect to p_1 and p_2 it appears that, if we choose $q_1 < \boldsymbol{\zeta}_{\min} = \mu^{-1}$, we can decrease the convergence factor by increasing p_1 because $\frac{\partial \rho_{\text{RR}}}{\partial p_1} < 0, \forall q_1 > \boldsymbol{\zeta}_{\min}$. A similar argument shows that $q_2 \leq \boldsymbol{\zeta}_{\max}$. This means that the optimized parameters $q_1^\star$ and $q_2^\star$ must satisfy

$$\mu^{-1} \leq q_1^\star < q_2^\star \leq \mu. \tag{4.3}$$

(4.2) and (4.3) imply that at $\boldsymbol{\zeta} = 1/\mu$, ρ_{RR} is an increasing function of p_1 and p_2 (or q_1 and q_2) while at $\boldsymbol{\zeta} = \mu$, ρ_{RR} is a decreasing function of p_1 and p_2 (or q_1 and q_2).

4.2. Extrema of ρ_{RR} with respect to $\boldsymbol{\zeta}$. The next step to solve (4.1) analytically is to find the location of the extrema of $\rho_{\text{RR}}(p_1, p_2, \boldsymbol{\zeta}, \gamma)$ with respect to $\boldsymbol{\zeta}$.

THEOREM 4.1 (Extrema of $\rho_{\text{RR}}(\boldsymbol{\zeta})$). *$\rho_{\text{RR}}(p_1, p_2, \boldsymbol{\zeta})$ has one or three positive local extrema. In the case of one extremum, it corresponds to a minimum and is located at $\chi = \sqrt{\frac{p_1 p_2}{2\gamma}}$.*

Proof. : We start by the following property that can easily be verified:

$$\rho_{\text{RR}}\left(p_1, p_2, \boldsymbol{\zeta}\right) = \rho_{\text{RR}}\left(p_1, p_2, \chi^2/\boldsymbol{\zeta}\right), \text{ where } \chi = \sqrt{\frac{p_1 p_2}{2\gamma}}$$

After derivation with respect to $\boldsymbol{\zeta}$, this leads to

$$\frac{\partial \rho_{\text{RR}}}{\partial \boldsymbol{\zeta}}(p_1, p_2, \boldsymbol{\zeta}) = -\frac{\chi^2}{\boldsymbol{\zeta}^2} \frac{\partial \rho_{\text{RR}}}{\partial \boldsymbol{\zeta}}(p_1, p_2, \chi^2/\boldsymbol{\zeta}) \tag{4.4}$$

which shows that $\frac{\partial \rho_{\text{RR}}}{\partial \boldsymbol{\zeta}}(p_1, p_2, \pm\chi) = 0$.

$\frac{\partial \rho_{\text{RR}}\left(p_1, p_2, \boldsymbol{\zeta}\right)}{\partial \boldsymbol{\zeta}}$ has the sign of $P(\boldsymbol{\zeta})$ a (unitary) sixth-order polynomial (the full expression of P is complicated and not given here). $P(\boldsymbol{\zeta})$ has thus either two or six real roots, among them $\boldsymbol{\zeta} = \chi$ is positive and $\boldsymbol{\zeta} = -\chi$ is negative. Let us suppose that $P(\boldsymbol{\zeta})$ has six real roots. We can show that only three of these six roots (including $\boldsymbol{\zeta} = \chi$) are positive. From (4.4) we see that if $\boldsymbol{\zeta}^0$ is a root of $P(\boldsymbol{\zeta})$, $\boldsymbol{\zeta}^1 = \chi^2/\boldsymbol{\zeta}^0$ is another one. Assuming that the four other roots are positive, we have

$$\boldsymbol{\zeta}_5 = -\chi \leq 0 \leq \boldsymbol{\zeta}_6 \leq \boldsymbol{\zeta}_1 \leq \boldsymbol{\zeta}_2 = \chi \leq \boldsymbol{\zeta}_3 (= \frac{\chi^2}{\boldsymbol{\zeta}_1}) \leq \boldsymbol{\zeta}_4 (= \frac{\chi^2}{\boldsymbol{\zeta}_6}),$$

and the sum of the six roots must be greater than 2χ and is therefore positive. However the sum of the six roots of $P(\boldsymbol{\zeta})$ is given by $-a_5$ where a_5 is the coefficient of the $\boldsymbol{\zeta}^5$ term and

is equal to $a_5 = \dfrac{(\gamma-1)(p_2-p_1)}{\gamma}$. Using the fact that $\gamma \geq 1$ and that (4.3) implies $p_2 \geq p_1$, $-a_5$ cannot be positive so that we conclude that we have at most three posivite roots for $P(\boldsymbol{\zeta})$. It can be verified that $P(0) < 0$ and $P(+\infty) > 0$ so that if only one positive root exists (at $\boldsymbol{\zeta} = \chi$), it is a local minimum. □

4.3. Equioscillation of ρ_{RR} at the end points. THEOREM 4.2 (Equioscillation at the end points). *The optimized convergence factor $\rho_{RR}(p_1^\star, p_2^\star, \zeta)$ satisfies*

- $\rho_{RR}(p_1^\star, p_2^\star, \chi) \leq \max\left(\rho_{RR}(p_1^\star, p_2^\star, \mu^{-1}), \rho_{RR}(p_1^\star, p_2^\star, \mu)\right)$ *with* $\chi = \sqrt{\frac{p_1^\star p_2^\star}{2\gamma}}$
- *the equioscillation property:* $\rho_{RR}(p_1^\star, p_2^\star, \mu^{-1}) = \rho_{RR}(p_1^\star, p_2^\star, \mu)$ *which holds only for* $p_1^\star p_2^\star = 2\gamma$

Proof. : We first demonstrate that $\rho_{\text{RR}}(p_1^\star, p_2^\star, \chi) \leq \max\left(\rho_{\text{RR}}(p_1^\star, p_2^\star, \mu^{-1}), \rho_{\text{RR}}(p_1^\star, p_2^\star, \mu)\right)$. If χ is the only positive root of $\dfrac{\partial \rho_{\text{RR}}(\boldsymbol{\zeta})}{\partial \boldsymbol{\zeta}}$, this is trivial since χ is a local minimum. Let's look at the case where there are three positive roots, in this case χ is a local maximum.

From the identity $\chi = \sqrt{\dfrac{p_1 p_2}{2\gamma}} = \sqrt{q_1 q_2}$ and (4.3) we get

$$1/\mu \leq q_1 \leq \chi = \sqrt{q_1 q_2} \leq q_2 \leq \mu \tag{4.5}$$

We already know that at $\boldsymbol{\zeta} = 1/\mu$, ρ_{RR} is a decreasing function of q_1 and that at $\boldsymbol{\zeta} = \mu$, ρ_{RR} is an increasing function of q_1. (4.5) shows that at $\boldsymbol{\zeta} = \chi$, ρ_{RR} is an increasing function of q_1 since $q_1 \leq \chi$. If we assume that $\rho_{\text{RR}}(p_1^\star, p_2^\star, \chi) \geq \rho_{\text{RR}}(p_1^\star, p_2^\star, \mu^{-1})$ then we can always decrease q_1 (or p_1) such that it improves the convergence factor (by reducing the values both at $\boldsymbol{\zeta} = \chi$ and at $\boldsymbol{\zeta} = \mu$). Playing with q_2 we can similarly prove that $\rho_{\text{RR}}(p_1^\star, p_2^\star, \chi) \leq \rho_{\text{RR}}(p_1^\star, p_2^\star, \mu)$. Note that this also demonstrates that $\boldsymbol{\zeta}_1 \geq 1/\mu$ and $\boldsymbol{\zeta}_3 \leq \mu$. This is sufficient to fully describe the behaviour of the convergence factor with respect to q_1, q_2 and $\boldsymbol{\zeta}$, as shown in Fig. 4.1. In practice, the two cases will be differentiated by the sign of the second-order derivative of $\rho_{\text{RR}}(p_1, p_2, \boldsymbol{\zeta})$ at $\boldsymbol{\zeta} = \chi$. The following proves that the values taken by

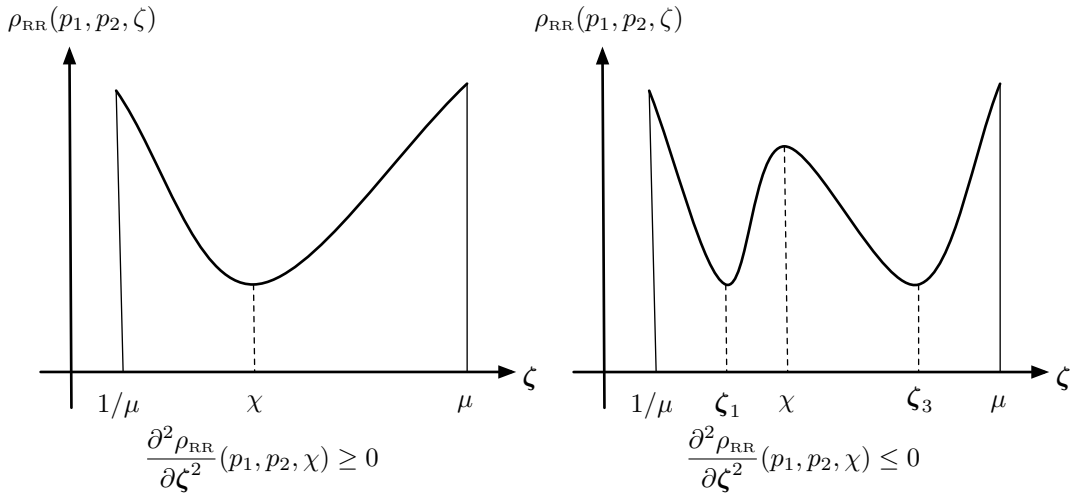

FIG. 4.1. *Behaviour of the convergence factor with respect to* $\boldsymbol{\zeta}$

$\rho_{\text{RR}}(p_1^\star, p_2^\star, \boldsymbol{\zeta})$ at the two end points $\boldsymbol{\zeta} = 1/\mu$, and $\boldsymbol{\zeta} = \mu$ are equal. Indeed if we consider

$\rho_{\text{RR}}(p_1, p_2, 1/\mu) < \rho_{\text{RR}}(p_1, p_2, \mu)$ (resp. $\rho_{\text{RR}}(p_1, p_2, 1/\mu) > \rho_{\text{RR}}(p_1, p_2, \mu)$), it is always possible to decrease the maximum value of $\rho_{\text{RR}}(\boldsymbol{\zeta})$ by increasing (resp. decreasing) the values of p_1 (resp. p_2). Thus the optimal parameters must satisfy $\rho_{\text{RR}}(p_1^\star, p_2^\star, \mu^{-1}) = \rho_{\text{RR}}(p_1^\star, p_2^\star, \mu)$: the equioscillation property.

This holds for

$$(p_1 + p_2)(2\gamma - p_1 p_2) S(p_1, p_2, \mu, \gamma) = 0 \tag{4.6}$$

with

$$\begin{aligned} S(p_1, p_2, \mu, \gamma) = 2\left[(1+\gamma^2) - \gamma(\mu + \mu^{-1})^2\right] p_1 p_2 + (\gamma - 1)(\mu + 1/\mu)(p_1 - p_2)(2\gamma + p_1 p_2) \\ + 2\gamma(p_1 - p_2)^2 - (2\gamma - p_1 p_2)^2 \end{aligned}$$

Obviously every couple (p_1, p_2) that satisfies the relation $p_1 p_2 = 2\gamma$ is solution to (4.6). We now show that there are no other admissible values. Other potential solutions of the problem are the solutions of $S(p_1, p_2, \mu) = 0$. S can be seen as a second-order polynomial in p_2 and thus has two real solutions:

$$p_2 = f_1(p_1) \qquad p_2 = f_2(p_1) \tag{4.7}$$

If we assume that p_2 is related to p_1 with one of the relations (4.7), looking at Fig. 4.1 we can argue that for any couple (p_1, p_2) we must have $\mathrm{d}p_2/\mathrm{d}p_1 < 0$ to satisfy an equioscillation property. Indeed let $\rho^\dagger_{\text{RR}}(p_1, \boldsymbol{\zeta})$ be defined as

$$\rho^\dagger_{\text{RR}}(p_1, \boldsymbol{\zeta}) = \rho_{\text{RR}}(p_1, p_2(p_1), \boldsymbol{\zeta})$$

Then

$$\frac{\partial \rho^\dagger_{\text{RR}}(p_1, \boldsymbol{\zeta})}{\partial p_1} = \frac{\partial \rho_{\text{RR}}(p_1, p_2(p_1), \boldsymbol{\zeta})}{\partial p_1} + \frac{\partial \rho_{\text{RR}}(p_1, p_2(p_1), \boldsymbol{\zeta})}{\partial p_2} \frac{\mathrm{d}p_2}{\mathrm{d}p_1} \tag{4.8}$$

We have already proved that the following properties must hold

$$\begin{aligned} &\frac{\partial \rho_{\text{RR}}(p_1, p_2(p_1), 1/\mu)}{\partial p_1} > 0, \frac{\partial \rho_{\text{RR}}(p_1, p_2(p_1), 1/\mu)}{\partial p_2} > 0 \\ &\frac{\partial \rho_{\text{RR}}(p_1, p_2(p_1), \mu)}{\partial p_1} < 0, \frac{\partial \rho_{\text{RR}}(p_1, p_2(p_1), \mu)}{\partial p_2} < 0 \end{aligned} \tag{4.9}$$

If we suppose $\mathrm{d}p_2/\mathrm{d}p_1 > 0$ then (4.8) and (4.9) show that $\rho^\dagger_{\text{RR}}(p_1, 1/\mu)$ is an increasing function of p_1 while $\rho^\dagger_{\text{RR}}(p_1, \mu)$ is a decreasing function of p_1. Hence, (4.9) and the equioscillation property cannot be satisfied at the same time if $\mathrm{d}p_2/\mathrm{d}p_1 > 0$. It can be shown that the two solutions given by (4.7) do not verify this last condition. Indeed one can prove that we have $\mathrm{d}f_1/\mathrm{d}p_1 > 0$ and $\mathrm{d}f_2/\mathrm{d}p_1 > 0$. Details of the computations are omitted here but we mention that the only conditions necessary to find this result are $\gamma > 0, \mu > 1$. We can conclude that $p_1 p_2 = 2\gamma$ is the only solution leading to an equioscillation property. □ It is worth mentioning that $\chi = \sqrt{\dfrac{p_1 p_2}{2\gamma}} = 1$ and that

$$\rho_{\text{RR}}(p_1^\star, p_2^\star, \boldsymbol{\zeta}) = \rho_{\text{RR}}(p_1^\star, p_2^\star, 1/\boldsymbol{\zeta}) \qquad \forall \boldsymbol{\zeta} \in [1/\mu, \mu]$$

4.4. Solution of the minmax problem. The convergence factor is now a function of p_1 and $\boldsymbol{\zeta}$ only:

$$\rho^{\dagger}_{\text{RR}}(p_1, \boldsymbol{\zeta}) = \rho_{\text{RR}}(p_1, 2\gamma/p1, \boldsymbol{\zeta})$$

LEMMA 4.3. *The solution of the minmax problem is given by the solution of the minimization of $\rho^{\dagger}_{RR}(p_1, 1/\mu)$. The minimization must be done under the constraint that $p_1^{\star} \geq p_1^{\star,\text{equi}}$ where $p_1^{\star,\text{equi}}$ is the solution of the three point equioscillation problem $\rho^{\dagger}_{RR}(p_1, 1) = \rho^{\dagger}_{RR}(p_1, 1/\mu) = \rho^{\dagger}_{RR}(p_1, \mu)$*
Thanks to Fig. 4.1 we can remark that the resolution of the minmax problem corresponds to the minimization of $\rho^{\dagger}_{\text{RR}}(p_1, 1/\mu)$ (or $\rho^{\dagger}_{\text{RR}}(p_1, \mu)$) with respect to p_1. If we are in the case where $\chi = 1$ is a local maximum, the additional constraint given by theorem (4.2) must be imposed

$$\rho^{\dagger}_{\text{RR}}(p_1, 1) \leq \rho^{\dagger}_{\text{RR}}(p_1, 1/\mu) \tag{4.10}$$

Knowing that $p_1 p_2 = 2\gamma$, or equivalently $q_1 q_2 = 1$, the range of admissible values given by (4.3) can now be written $1/\mu \leq q_1 \leq 1$ and translates in terms of the variable p_1:

$$p_1 \in [p_{1,\min}, p_{1,\max}] \text{ where } p_{1,\min} = (1 - \gamma + \sqrt{1+\gamma^2})/\mu,\ p_{1,\max} = (1 - \gamma + \sqrt{1+\gamma^2}) \tag{4.11}$$

Moreover it can be shown that $\rho^{\dagger}_{\text{RR}}(p_1, 1)$ is a decreasing function of p_1 and therefore the constraint (4.10) can also be written $p_1^{\star} \geq p_1^{\star,\text{equi}}$ where $p_1^{\star,\text{equi}}$ is the solution of a three point equioscillation problem $\rho^{\dagger}_{\text{RR}}(p_1^{\star,\text{equi}}, 1) = \rho^{\dagger}_{\text{RR}}(p_1^{\star,\text{equi}}, 1/\mu) (= \rho^{\dagger}_{\text{RR}}(p_1^{\star,\text{equi}}, \mu))$.

We now look at the minimization of $\rho^{\dagger}_{\text{RR}}(p_1, 1/\mu)$ for $p_1 \in [p_{1,\min}, p_{1,\max}]$.

LEMMA 4.4. *For $\gamma > 1$, the derivative of $\rho^{\dagger}_{RR}(p_1, 1/\mu)$ has exactly one root in the range $[p_{1,\min}, p_{1,\max}]$. This root corresponds to a local minimum of $\rho^{\dagger}_{RR}(p_1, 1/\mu)$. In the special case $\gamma = 1$, $p_1 = p_{1,\max} (= \sqrt{2})$ is always a root of $\dfrac{\partial \rho^{\dagger}_{RR}}{\partial p_1}(p_1, 1/\mu)$.* The derivative of $\rho^{\dagger}_{\text{RR}}(p_1, 1/\mu)$ can be written as

$$\frac{\partial \rho^{\dagger}_{\text{RR}}}{\partial p_1}(p_1, 1/\mu) = g(p_1, \mu) N(p_1, \mu)$$

where g is a strictly positive function and $N(p_1, \mu)$ a sixth-order polynomial in p_1. The change of variable $v = 2\gamma/p1 - p1$ transforms $N(p_1, \mu)$ in

$$N(p_1, \mu) = p_1^3 Q(v)$$

where $Q(v)$ is the third-order polynomial given by

$$Q(v) = 8(\gamma - 1)(1 + \gamma^2) + 2\beta(\gamma\beta^2 - 3(1 + \gamma^2))v + 2(\gamma - 1)\beta^2 v^2 - \beta v^3 \tag{4.12}$$

with $\beta = 1/\mu + \mu$.
It can be shown that, for $\gamma > 1$, this polynomial has only one root in $[v_{\min}, v_{\max}]$ where, according to (4.11), $v_{\min}$ and $v_{\max}$ are given by

$$v_{\min} = 2(\gamma - 1),\ v_{\max} = (\gamma - 1)\beta + \sqrt{1+\gamma^2}\sqrt{\beta^2 - 4} \tag{4.13}$$

This root corresponds to a minimum of $\rho^{\dagger}_{\text{RR}}(p_1, 1/\mu)$ since it can be found that $\dfrac{\partial \rho^{\dagger}_{\text{RR}}}{\partial p_1}(p_{1,\min}, 1/\mu) \leq 0$ and $\dfrac{\partial \rho^{\dagger}_{\text{RR}}}{\partial p_1}(p_{1,\max}, 1/\mu) \geq 0$. For $\gamma = 1$, $v = v_{\min} = 0$ (i.e., $p_1 = p_{1,\max} = \sqrt{2}$) is always

a root of $Q(v)$. Fig. 4.2 illustrates the variations of $\rho^{\dagger}_{\text{RR}}(p_1, 1/\mu)$ with p_1. $p_1^{\min}$ is the location of the minimum of $\rho^{\dagger}_{\text{RR}}(p_1, 1/\mu)$ over $[p_{1,\min}, p_{1,\max}]$. The solution of the constrained

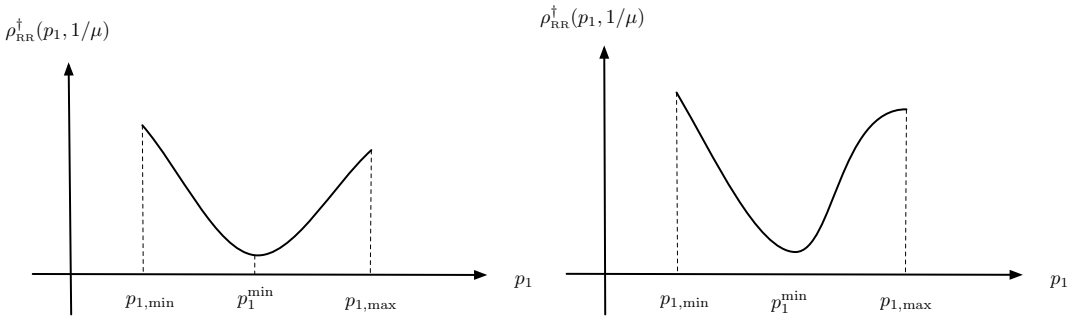

FIG. 4.2. *Behaviour of $\rho^{\dagger}_{RR}(p_1, 1/\mu)$ with respect to p_1. The general case ($\gamma > 1$) is on the left and the special case $\gamma = 1$ on the right*

minimization problem is now easily handled: if $p_1^{\min} \leq p_1^{\star,\text{equi}}$ the solution of the minmax problem is given by $p_1^{\star,\text{equi}}$, otherwise the solution of the minmax problem is given by $p_1^{\min}$. The inequality $p_1^{\min} \leq p_1^{\star,\text{equi}}$ is satisfied if and only if $\dfrac{\partial \rho^{\dagger}_{\text{RR}}}{\partial p_1}(p_1^{\star,\text{equi}}, \mu) \geq 0$ or equivalently $Q(v^{\star,\text{equi}}) \geq 0$ (where $v^{\star,\text{equi}} = 2\gamma/p_1^{\star,\text{equi}} - p_1^{\star,\text{equi}}$).

Finaly the following result is useful: for $v \geq v_{\max}$ or equivalently $p_1 \leq p_{1,\min}$ we have $Q(v) \leq 0$ $\left(\text{or } \dfrac{\partial \rho^{\dagger}_{\text{RR}}(p_1, 1/\mu)}{\partial p_1} \leq 0\right)$. Indeed, using relation (4.8) at $\boldsymbol{\zeta} = 1/\mu$:

$$\frac{\partial \rho^{\dagger}_{\text{RR}}(p_1, 1/\mu)}{\partial p_1} = \frac{\partial \rho_{\text{RR}}(p_1, p_2(p_1), 1/\mu)}{\partial p_1} + \frac{\partial \rho_{\text{RR}}(p_1, p_2(p_1), 1/\mu)}{\partial p_2} \frac{\mathrm{d}p_2}{\mathrm{d}p_1}$$

If $p_1 \leq p_{1,\min}$, $\dfrac{\partial \rho_{\text{RR}}(p_1, p_2(p_1), 1/\mu)}{\partial p_1} < 0$, but the relation $p_2 = 2\gamma/p_1$ implies $p_2 \geq p_{2,\max}$ $\left(= \left(\gamma - 1 + \sqrt{1+\gamma^2}\right)\mu\right)$ so that $\dfrac{\partial \rho_{\text{RR}}(p_1, p_2(p_1), 1/\mu)}{\partial p_2} \geq 0$. Using $\dfrac{\mathrm{d}p_2}{\mathrm{d}p_1} = -2\gamma/p_1^2 \leq 0$, this proves that $\dfrac{\partial \rho^{\dagger}_{\text{RR}}(p_1, 1/\mu)}{\partial p_1} \leq 0$.

We are now done with the problem of finding the solution of the three point equioscillation problem.

THEOREM 4.5 (Equioscillation between 3 points). *The only parameters $p_1^{\star,\text{equi}}$ and $p_2^{\star,\text{equi}}$, such that $p_1^{\star,\text{equi}} \leq p_{1,\max}$, that satisfy an equioscillation of the convergence factor ρ_{RR} between the three points $(1/\mu, 1, \mu)$ are*

$$\begin{cases} p_1^{\star,\text{equi}} = \dfrac{1}{2}\left[-v^{\star,\text{equi}} + \sqrt{8\gamma + (v^{\star,\text{equi}})^2}\right] \\ p_2^{\star,\text{equi}} = 2\gamma \left(p_1^{\star,\text{equi}}\right)^{-1} \end{cases}$$

where

$$v^{\star,\text{equi}} = \frac{1}{2}\left[(2+\beta)(\gamma-1) + \sqrt{4(1+\gamma)^2(\beta-1) + \beta^2(\gamma-1)^2}\right] \tag{4.14}$$

Proof. : We have to find the solution of the problem $\rho^{\dagger}_{\text{RR}}(p_1, 1/\mu) = \rho^{\dagger}_{\text{RR}}(p_1, 1)$. It can be shown that this is equivalent to the search of the zeros of a fourth-order polynomial $R(p_1)$ that can be written under the form

$$R(p_1) = p_1^2 T(v), \quad T(v) = 2(1+\gamma^2) - 4\gamma\beta + (1-\gamma)(2+\beta)v + v^2$$

where v is again defined by $v = 2\gamma/p_1 - p_1$. The unique root of $T(v)$ that satisties $v \geq v_{\min}$ (i.e., $p_1 \leq p_{1,\max}$) is given by

$$v^{\star,\text{equi}} = \frac{1}{2}\left[(2+\beta)(\gamma-1) + \sqrt{4(1+\gamma)^2(\beta-1) + \beta^2(\gamma-1)^2}\right]$$

and $p_1^{\star,\text{equi}}$ is deduced from the relation between p_1 and v. □

Putting everything together the solution of the minmax problem is given by

THEOREM 4.6. *The analytical solution $\lambda_1^{0,\star}$ and $\lambda_2^{0,\star}$ of the minmax problem*

$$\min_{\lambda_1^0, \lambda_2^0 \in \mathbb{R}} \left(\max_{\omega \in [\omega_{\min}, \omega_{\max}]} \rho_{RR}(\lambda_1^0, \lambda_2^0, D_1, D_2, \omega) \right)$$

is given by

$$\begin{cases} \lambda_1^{0,\star} = \dfrac{\sqrt{D_1}\,(\omega_{\min}\omega_{\max})^{1/4}}{2\sqrt{2}} \left[-v^\star + \sqrt{8\gamma + (v^\star)^2}\right] \\ \lambda_2^{0,\star} = \sqrt{D_1 D_2}\sqrt{\omega_{\min}\omega_{\max}}/\lambda_1^{0,\star} \end{cases}$$

where

$$v^\star = \begin{cases} v^{\star,\text{equi}} & \text{if } Q(v^{\star,\text{equi}}) \geq 0 \\ v^{\star,\text{mini}} & \text{else} \end{cases}$$

with $v^{\star,\text{equi}}$ given by (4.14). $v^{\star,\text{mini}}$ is the unique solution of $Q(v) = 0$ over $[v_{\min}, v_{\max}]$.

Proof. : All the proof ingredients are given before. Note that $v^{\star,\text{equi}}$ may be larger than $v_{\max}$. However since we have proved that $Q(v \geq v_{\max}) \leq 0$, this case does not have to be explicitly considered. Substitution of γ and μ by their respective expressions, and multiplication of $p_1^\star$ and $p_2^\star$ by $\sqrt{\zeta_{\min}\zeta_{\max}/2}$ lead to the expected result for $\lambda_1^{0,\star}$ and $\lambda_2^{0,\star}$ with respect to D_1, D_2, $\omega_{\min}$, and $\omega_{\max}$. □

Note that this additional result can also be shown :

$$Q(v^{\star,\text{equi}}) \geq 0 \Leftrightarrow \beta \geq 1+\sqrt{5} \text{ or } \left(\beta^0 < \beta < 1+\sqrt{5} \text{ and } \gamma \geq f(\beta)\right) \tag{4.15}$$

where β^0 is the root of the fourth-order polynomial $16 - 16X - 4X^2 + X^4$ whose approximate value is given by $\beta^0 \approx 2.77294$ and f is given by

$$f(\beta) = \frac{(\beta-2)^3\beta(\beta+2) + (4+2\beta-\beta^2)\sqrt{-16+48\beta-44\beta^2+12\beta^3+3\beta^4-4\beta^5+\beta^6}}{16-16\beta-4\beta^2+\beta^4}$$

$f(\beta)$ for $\beta^0 < \beta < 1+\sqrt{5}$ is plotted on Fig. 4.3. We can remark that $f(\beta) \geq 1,\ \forall\beta$ so that the condition $\gamma \geq f(\beta)$ is always false for $\gamma = 1$ (continuous case).

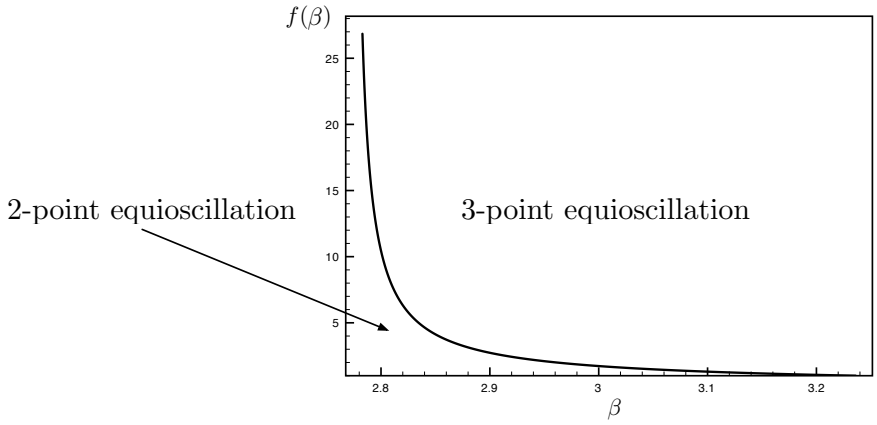

FIG. 4.3. *Transition from a 2 point to a 3 point equioscillation for $\beta^0 < \beta < 1+\sqrt{5}$. The 3 point equioscillation occurs when $\gamma \geq f(\beta)$.*

It is also interesting to know if $\chi = \sqrt{\frac{p_1 p_2}{2\gamma}} = 1$ is either a local minimum or a local maximum of the optimized convergence factor by looking at the sign of $\dfrac{\partial^2 \rho^{\dagger}_{\text{RR}}}{\partial \chi^2}(p_1, \chi)$. It can be proved that in terms of the variable $v = 2\gamma/p_1 - p_1$, the inequality $\dfrac{\partial^2 \rho^{\dagger}_{\text{RR}}}{\partial \chi^2}(p_1, \chi) > 0$ can be written:

$$v \geq v_0, \qquad \text{where } v_0 = 2(\gamma - 1) + \sqrt{2(1+\gamma^2)}$$

We deduce that $\boldsymbol{\zeta} = \chi = 1$ is a local minimum only if $v^{\star,\text{mini}} \leq v_0$. This can be checked by evaluating the polynomial $Q(v)$ at $v = v_0$ and looking at the sign of the result: if $Q(v_0) \leq 0$ then $v^{\star,\text{mini}} \leq v_0$ and we have a local minimum at $\boldsymbol{\zeta} = \chi = 1$.
It can be found that

$$Q(v_0) < 0 \Leftrightarrow 2 < \beta < \beta_0 \qquad \text{or } \left(\beta_0 \leq \beta \leq 2\sqrt{2} \text{ and } \gamma < g(\beta)\right)$$

where $\beta_0 = \dfrac{8+5\sqrt{2}}{2\left(3+2\sqrt{2}\right)} + \dfrac{\sqrt{90+64\sqrt{2}}}{2\left(3+2\sqrt{2}\right)} \approx 2.44547$. The analytical expression of $g(\beta)$ is complicated and is not given here. Note that $g(\beta) \geq 1, \ \forall \beta$ so that for the special case $\gamma = 1$, $Q(v_0) < 0$ is equivalent to $2 < \beta \leq 2\sqrt{2}$.
Fig. 4.4 summarizes the three different domains: 3 point equioscillation, 2 point equioscillation with χ as a local maximum and 2 point equioscillation with χ as a local minimum.
The resulting optimized convergence factor is shown in Fig. 4.5 with respect to μ and γ.
We can draw the following remarks about the convergence properties of the Schwarz algorithms : the convergence speed increases when the discontinuities of the coefficients (γ) is increased and the convergence speed decreases when μ, an increasing function of the ratio $\dfrac{\omega_{\max}}{\omega_{\min}}$, is increased. In Fig. 4.6 we compare, for $\mu = 2$ and $\mu = 6$, the results found in the optimized two-sided case with the optimized *Robin-Neumann* transmission conditions (found in Sec. 3). The *Robin-Robin* approach is significantly more efficient than the *Robin-Neumann* approach when γ is close to one. When γ is increased, both tends towards a *Dirichlet-Neumann* operator.

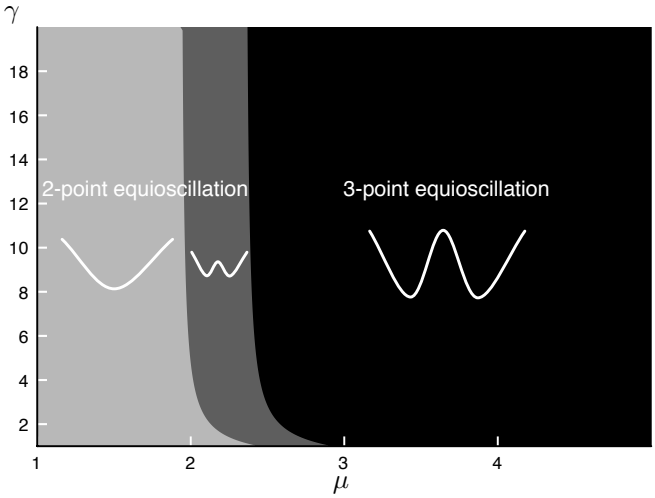

FIG. 4.4. *The three different domains of three point equioscillation (black), two point equioscillation with χ being a local maximum (dark grey) and two point equioscillation with χ being a local minimum (light grey)*

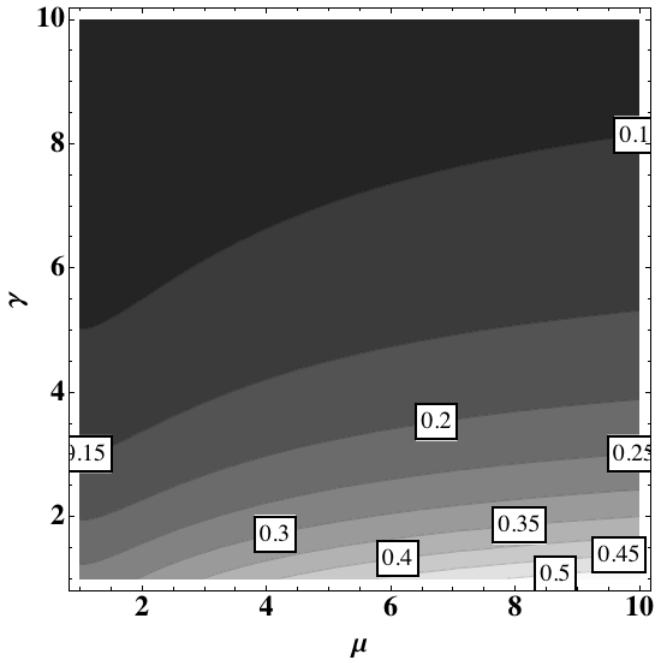

FIG. 4.5. *Optimized convergence factor with respect to μ and γ ($1 \leq \mu \leq 10, 1 \leq \gamma \leq 10$)*

THEOREM 4.7 (Asymptotic performance). *For $D_2 > D_1$ (i.e., $\gamma > 1$), $\omega_{\max} = \dfrac{\pi}{\Delta t}$, and Δt goes to zero, the optimal Robin parameters given by Theorem 4.6 are*

$$\lambda_1^{0,\star} \approx \lambda_1^{0,(\mathrm{as})} = \sqrt{2D_1}\left(\frac{\gamma}{\gamma-1}\sqrt{\omega_{\min}} - 2\gamma\frac{\gamma^2+1}{(\gamma-1)^3\pi^{1/4}}\omega_{\min}^{3/4}\Delta t^{1/4}\right)$$

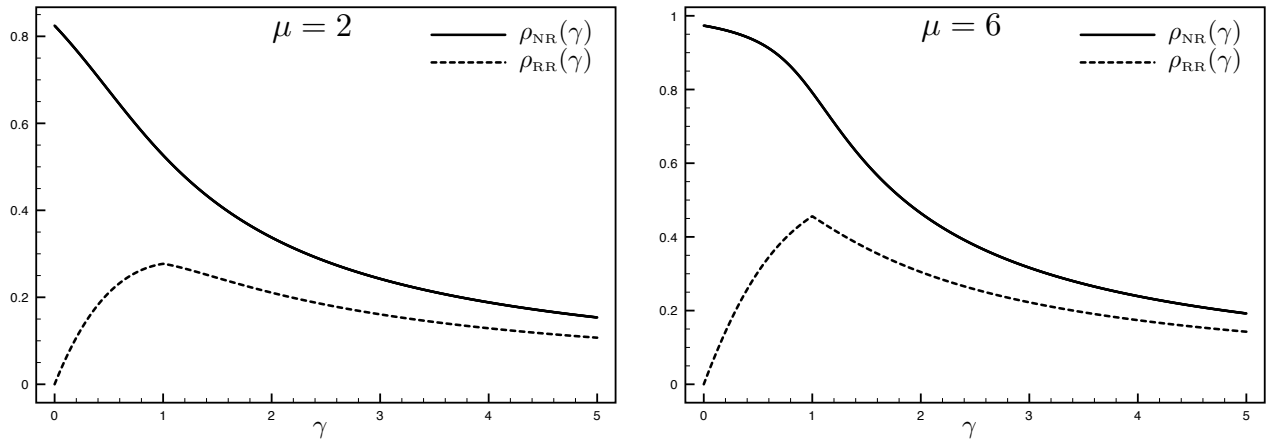

FIG. 4.6. *Optimized convergence factors for Neumann-Robin and Robin-Robin boundary conditions.* $\mu = 2$ *(left) and* $\mu = 6$ *(right)*

$$\lambda_2^{0,\star} \approx \lambda_2^{0,(\mathrm{as})} = \sqrt{2D_1}\left(\frac{\gamma-1}{2}\sqrt{\pi}\Delta t^{-1/2} + \frac{\gamma^2+1}{\gamma-1}(\pi\omega_{\min})^{1/4}\Delta t^{-1/4}\right)$$

and the asymptotic convergence of the optimized two-sided Robin-Robin algorithm is

$$\max_{\omega_{\min}\leq\omega\leq\frac{\pi}{\Delta t}} \rho_{RR}(\lambda_1^{0,\star},\lambda_2^{0,\star},\omega) = \frac{1}{\gamma}\left(1 - 2\frac{(\gamma+1)}{(\gamma-1)}\left(\frac{\omega_{\min}}{\pi}\right)^{1/4}\Delta t^{1/4}\right) + O(\Delta t^{1/2})$$

Note that those asymptotic results are obtained by assuming that $v^\star = v^{\star,\mathrm{equi}}$, which is always the case when $\Delta t \to 0$ (i.e., $\mu \to \infty$), as shown by (4.15). The optimized Robin-Robin conditions lead to an asymptotic convergence factor of the form $\sqrt{D_1/D_2}\left(1 - O(\Delta t^{1/4})\right)$ for small Δt and $D_1 < D_2$. The associated algorithm is thus less sensitive to Δt than the Neumann-Robin algorithm. However, the asymptotic Robin parameters given in Theorem 4.7 must be used with caution as they degenerate when $\gamma \to 1$, as well as when $\Delta t \gg 0$ (in this case $\lambda_1^{0,(\mathrm{as})}$ can become negative). It is worth mentioning that the asymptotic bound on the optimized convergence factor given in Theorem 4.7 shows that the optimized Robin-Robin conditions will always be more efficient than Dirichlet-Neumann conditions. Indeed, it can easily be checked that the multiplying term $1/\gamma$ in front of the bound correspond to the convergence factor of the Dirichlet-Neumann algorithm.

Furthermore, we can not directly compare this result with the one obtained in [10] for the advection-diffusion-reaction equation. The latter study is done by assuming $\omega_{\min} = 0$ and as a result of this assumption their optimized parameter, when canceling the advection and reaction coefficients, are simply $\lambda_1^{0,\star} = \lambda_2^{0,\star} = 0$. Indeed, one can easily find that for a diffusion problem the low frequency approximation λ_j^{low} of the absorbing conditions λ_j^{opt}, given in (2.7), for $\omega_{\min} \to 0$ is indeed $\lambda_j^{\mathrm{low}} = 0$.

4.5. The continuous case. Because the two-sided Robin-Robin case with continuous diffusion coefficients has never been studied in the literature we now provide the results in this particular case.

THEOREM 4.8 (Continuous case). *Under the assumption $D_1 = D_2 = D$, the optimal parameters $\lambda_1^{0,\star}$ and $\lambda_2^{0,\star}$ are given by*

$$\begin{cases} \lambda_1^{0,\star} = \dfrac{\sqrt{D}\,(\omega_{\min}\omega_{\max})^{1/4}}{2\sqrt{2}}\left[-v^\star + \sqrt{8+(v^\star)^2}\right] \\ \lambda_2^{0,\star} = \dfrac{\sqrt{D}\,(\omega_{\min}\omega_{\max})^{1/4}}{2\sqrt{2}}\left[\ v^\star + \sqrt{8+(v^\star)^2}\right] \end{cases}$$

where

$$v^\star = \begin{cases} 2\sqrt{\beta-1} & \text{if } \beta \geq 1+\sqrt{5} \\ \sqrt{2\beta^2-12} & \text{if } \sqrt{6} \leq \beta < 1+\sqrt{5} \\ 0 & \text{if } 2 < \beta < \sqrt{6} \end{cases}$$

with $\beta = \dfrac{\sqrt{\omega_{\max}}+\sqrt{\omega_{\min}}}{(\omega_{\min}\omega_{\max})^{1/4}}$.

Proof. : We use theorem (4.6) which gives the optimal conditions in the general case. As already mentioned the condition $Q(v^{\star,\text{equi}}) \geq 0$ reduces for $\gamma = 1$ to $\beta \geq 1+\sqrt{5}$. In that case, the solution of the minmax problem is given by $v^\star = v^{\star,\text{equi}} = 2\sqrt{\beta-1}$. If $\beta < 1+\sqrt{5}$, we have to compute $v^{\star,\min}$ the value that cancels $Q(v)$ over $[v_{\min}, v_{\max}]$ where $v_{\min} = 0$, $v_{\max} = 2\sqrt{\beta^2-4}$. For $\gamma = 1$, the expression (4.12) of the polynomial $Q(v)$ is

$$Q(v) = -\beta v\left(v^2 - (2\beta^2-12)\right)$$

We find that

$$v^{\star,\min} = \begin{cases} \sqrt{2\beta^2-12} & \text{if } \beta \geq \sqrt{6} \\ 0 & \text{if } 2 < \beta \leq \sqrt{6} \end{cases}$$

Note that when $\beta \leq \sqrt{6}$ we get $v^\star = 0$. This implies $\lambda_1^{0,\star} = \lambda_2^{0,\star} = \sqrt{D_1}\,(\omega_{\min}\omega_{\max})^{1/4}$, which corresponds to the zeroth-order *one-sided* optimal parameters found in [8]. ∎

5. Numerical experiments with two subdomains. The model problem (2.2) is discretized using a backard Euler scheme in time and a second-order scheme on a staggered grid in space. For the interior points the scheme is

$$\frac{u_k^{n+1}-u_k^n}{\Delta t} = \frac{1}{x_{k+\frac{1}{2}}-x_{k-\frac{1}{2}}}\left[\mathrm{F}_{k+\frac{1}{2}}^{n+1} - \mathrm{F}_{k-\frac{1}{2}}^{n+1}\right] \tag{5.1}$$

with $\mathrm{F}_{k+\frac{1}{2}}^n = D_{k+\frac{1}{2}}\dfrac{u_{k+1}^n-u_k^n}{x_{k+1}-x_k}$. Note that for practical applications the use of the Crank-Nicolson scheme in time is avoided because this scheme leads to unphysical behaviour. Indeed, unlike the backward Euler scheme, the Crank-Nicolson scheme fails to satisfy the so-called *monotonic damping* property [21]. We decompose the computational domain Ω into two non-overlapping subdomains $\Omega_1 = [-L_1, 0]$ and $\Omega_2 = [0, L_2]$, with $L_1 = L_2 = 500$ m. An homogeneous Neumann boundary condition is imposed at $x = -L_1$ and $x = L_2$. As it is usually done in numerical models, the resolution Δx_k is progressively refined to enhance the resolution in the boundary layers in the vicinity of the air-sea interface. We use $N = 75$ points in each subdomain and the resolution varies from $\Delta x_k = 25$ m at $x = L_1$ (resp.

$x = L_2$) to $\Delta x_k = 1$ m at $x = 0$. The Robin condition $g_{N+\frac{1}{2}}$ on the interface Γ (located at $x = x_{N+\frac{1}{2}}$ on Ω_1 and at $x = x_{\frac{1}{2}}$ on Ω_2) is discretized by assuming that the flux F is constant on the first cell near Γ. This leads to

$$g_{N+\frac{1}{2}} = D_{N-\frac{1}{2}} \frac{u_N - u_{N-1}}{x_{N-\frac{1}{2}} - x_{N-\frac{3}{2}}} + \lambda u_N, \tag{5.2}$$

where λ is the Robin parameter. We simulate directly the error equations; i.e., $f_1 = f_2 = 0$ in (2.2) and $u_0(x) = 0$. We start the iteration with a random initial guess $u_2^0(0,t)$ ($t \in [0,T]$) so that it contains a wide range of the temporal frequencies that can be resolved by the computational grid. We perform simulations for four different types of transmission conditions at $x = 0$: Dirichlet-Neumann (DN), optimized Neumann-Robin (NR*), optimized Robin-Robin (RR*), and asymptotically optimized Robin-Robin (RR$^{(\mathrm{as})}$). In Fig. 5.1 we show the evolution of the $\mathcal{L}^\infty$-norm of the error obtained for those four cases for $\gamma = 10^{\frac{1}{4}} \approx 1.7783$, $\gamma = \sqrt{10} \approx 3.1623$, and $\gamma = 10$, with $\mu = 6$ and $\mu = 12$. We choose $\Delta t = 100$ s, $D_2 = 0.5$ m^2 s^{-1}, D_1 is then deduced depending on the value of γ. As expected, we get the best results with the two-sided Robin conditions. Consistent with Fig. 4.5 the convergence is faster when γ is large and when μ is small. Moreover, when the discontinuity γ between the diffusion coefficients is increased the algorithm becomes less and less sensitive to the choice of transmission conditions and to the parameter μ. The asymptotic optimized Robin-Robin conditions provide a good approximation of the optimized Robin-Robin conditions, even for $\Delta t = 100$ s $\gg 0$. Those conditions are especially efficient when γ is sufficiently larger than 1. Finally, we remark that the optimized Neumann-Robin conditions provide only a slight improvement compared to the classical Dirichlet-Neumann conditions.

Conclusion. In this paper, we obtain new results for an optimized Schwarz method defined on non-overlapping diffusion problems with discontinuous coefficients. This method uses zeroth-order two-sided Robin transmission conditions; i.e., we consider two different Robin conditions on each side of the interface. We base our approach on a model problem with two subdomains and we prove the convergence of the corresponding algorithm. Then we analytically study the behavior of the convergence factor with respect to the parameters of the problem. We show that the optimized convergence factor satisfies an equioscillation property between two or three points depending on the parameter values. In comparison with other methods using the Neumann-Robin or Dirichlet-Neumann conditions, these two-sided Robin-Robin conditions are significantly more efficient, especially when the ratio between the discontinuous coefficients is close to one. Asymptotic results for Δt small are given. Numerical results show the performance of the different type of transmission conditions introduced in this paper. Those results are consistent with the analytical study.

Acknowledgements. This research was partially supported by the French National Research Agency (ANR) project "COMMA" and by the INRIA project-team MOISE.

REFERENCES

[1] D. Bennequin, M. Gander, and L. Halpern, *Optimized Schwarz waveform relaxation methods for convection reaction diffusion problems*, Technical Report 2004-24, LAGA, Université Paris 13, 2004.

[2] D. Bennequin, M. J. Gander, and L. Halpern, *A homographic best approximation problem with application to optimized Schwarz waveform relaxation*, Math. Comp., 78 (2009), pp. 185–223.

[3] E. Blayo, L. Halpern, and C. Japhet, *Optimized Schwarz waveform relaxation algorithms with nonconforming time discretization for coupling convection-diffusion problems with discontinuous coefficients*, in Domain decomposition methods in science and engineering XVI, vol. 55 of Lect. Notes Comput. Sci. Eng., Springer, Berlin, 2007, pp. 267–274.

[4] G. Danabasoglu, W. G. Large, J. J. Tribbia, P. R. Gent, B. P. Briegleb, and J. C. McWilliams, *Diurnal coupling in the tropical oceans of ccsm3*, Journal of Climate, 19 (2006), pp. 2347–2365.

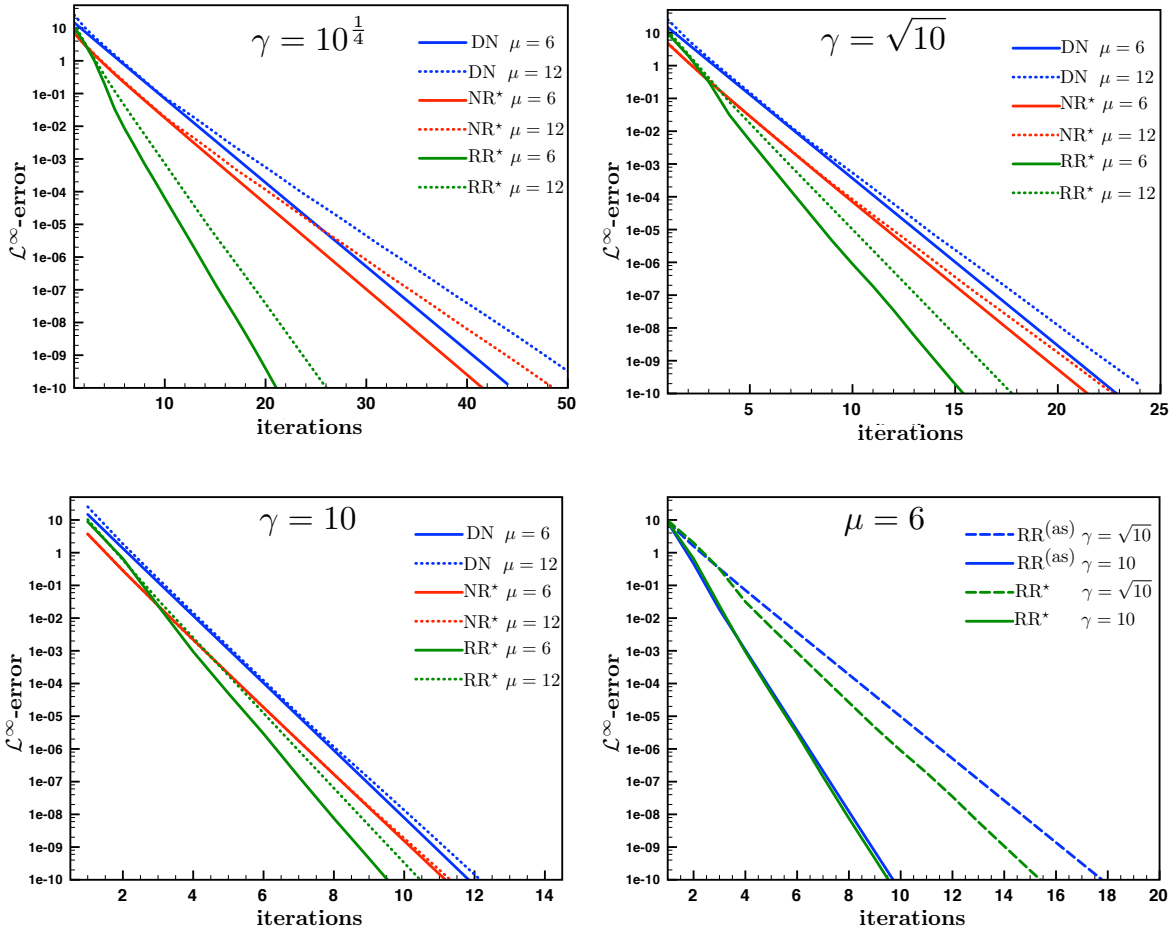

FIG. 5.1. *Convergence for $\gamma = 10^{\frac{1}{4}}$ (top,left), $\gamma = \sqrt{10}$ (top,right), and $\gamma = 10$ (bottom, left) for $\mu = 6$ and $\mu = 12$ in the DN, RR* and NR* cases. Comparison between RR* and RR$^{(\mathrm{as})}$ (bottom, right).*

[5] V. F. DEM'YANOV AND V. N. MALOZEMOV, *On the theory of non-linear minimax problems*, Russian Mathematical Surveys, 26 (1971), p. 57.

[6] O. DUBOIS, *Optimized Schwarz methods for the advection-diffusion equation and for problems with discontinuous coefficients*, ProQuest LLC, Ann Arbor, MI, 2007. Thesis (Ph.D.)–McGill University (Canada).

[7] M. J. GANDER, *Schwarz methods over the course of time*, Electron. Trans. Numer. Anal., 31 (2008), pp. 228–255.

[8] M. J. GANDER AND L. HALPERN, *Methodes de relaxation d'ondes pour l'equation de la chaleur en dimension 1*, C. R. Acad. Sci. Paris, 336 (2003), pp. 519–524.

[9] ———, *Optimized Schwarz waveform relaxation methods for advection reaction diffusion problems*, SIAM J. Numer. Anal., 45 (2007), pp. 666–697 (electronic).

[10] M. J. GANDER, L. HALPERN, AND M. KERN, *A Schwarz waveform relaxation method for advection-diffusion-reaction problems with discontinuous coefficients and non-matching grids*, in Domain decomposition methods in science and engineering XVI, vol. 55 of Lect. Notes Comput. Sci. Eng., Springer, Berlin, 2007, pp. 283–290.

[11] M. J. GANDER, L. HALPERN, AND F. MAGOULÈS, *An optimized Schwarz method with two-sided Robin transmission conditions for the Helmholtz equation*, Internat. J. Numer. Methods Fluids, 55 (2007), pp. 163–175.

[12] M. J. GANDER, L. HALPERN, AND F. NATAF, *Optimal convergence for overlapping and non-overlapping*

Schwarz waveform relaxation, in Eleventh International Conference on Domain Decomposition Methods (London, 1998), DDM.org, Augsburg, 1999, pp. 27–36 (electronic).

[13] M. J. GANDER AND A. M. STUART, *Space-time continuous analysis of waveform relaxation for the heat equation*, SIAM J. Sci. Comput., 19 (1998), pp. 2014–2031.

[14] C. JAPHET AND F. NATAF, *The best interface conditions for domain decomposition methods: absorbing boundary conditions*, in Absorbing boundaries and layers, domain decomposition methods, Nova Sci. Publ., Huntington, NY, 2001, pp. 348–373.

[15] E. LELARASMEE, A. RUEHLI, AND A. SANGIOVANNI-VINCENTELLI, *The waveform relaxation method for time-domain analysis of large scale integrated circuits*, Computer-Aided Design of Integrated Circuits and Systems, IEEE Transactions on, 1 (1982), pp. 131 – 145.

[16] F. LEMARIÉ, *Algorithmes de Schwarz et couplage océan-atmosphére*, 2008. Thesis (Ph.D.)–Joseph Fourier University (France).

[17] F. LEMARIÉ, L. DEBREU, AND E. BLAYO, *Toward an optimized global-in-time schwarz algorithm for diffusion equations with discontinuous and spatially variable coefficients, part 2 : the variable coefficients case*, Electron. Trans. Numer. Anal., (2011). Under review.

[18] P.-L. LIONS, *On the Schwarz alternating method. III. A variant for nonoverlapping subdomains*, in Third International Symposium on Domain Decomposition Methods for Partial Differential Equations (Houston,TX, 1989), SIAM, Philadelphia, PA, 1990, pp. 202–223.

[19] Y. MADAY AND F. MAGOULÈS, *Non-overlapping additive Schwarz methods tuned to highly heterogeneous media*, C. R. Math. Acad. Sci. Paris, 341 (2005), pp. 701–705.

[20] O. S. MADSEN, *A realistic model of the wind-induced ekman boundary layer*, Journal of Physical Oceanography, 7 (1977), pp. 248–255.

[21] G. MANFREDI AND M. OTTAVIANI, *Finite-difference schemes for the diffusion equation*, in Dynamical Systems, Plasmas and Gravitation, P. Leach, S. Bouquet, J.-L. Rouet, and E. Fijalkow, eds., vol. 518 of Lecture Notes in Physics, Springer Berlin / Heidelberg, 1999, pp. 82–92.

[22] J. C. MCWILLIAMS, *Irreducible imprecision in atmospheric and oceanic simulations*, Proceedings of the National Academy of Sciences, 104 (2007), pp. 8709–8713.